

UG-FT-137/02
CAFPE-7/02
hep-ph/0207328
July 2002

Lepton Flavor Violation in Z and Lepton Decays in Supersymmetric Models

J. I. ILLANA AND M. MASIP

*Centro Andaluz de Física de Partículas Elementales (CAFPE) and
Departamento de Física Teórica y del Cosmos
Universidad de Granada
E-18071 Granada, Spain*

Abstract

The observation of charged lepton flavor non-conservation would be a clear signature of physics beyond the Standard Model. In particular, supersymmetric (SUSY) models introduce mixings in the sneutrino and the charged slepton sectors which could imply flavor-changing processes at rates accessible to upcoming experiments. In this paper we analyze the possibility to observe $Z \rightarrow \ell_I \ell_J$ in the GigaZ option of DESY TESLA. We show that if GigaZ reaches its best projected sensitivity it could observe $Z \rightarrow \tau e; \tau \mu$ consistently with present bounds on $\tau \rightarrow e\gamma; \mu\gamma$. However, although models with SUSY masses above the current limits could predict a branching ratio $\text{BR}(Z \rightarrow \mu e)$ accessible to the experiment, they would then imply an unobserved rate of $\mu \rightarrow e\gamma$ and thus are excluded. We update the limits from $\ell_J \rightarrow \ell_I \gamma$ on the slepton mass insertions $\delta_{LL,RR,LR}$ and discuss the correlation between flavor changing and $g_\mu - 2$ in SUSY models.

1 Introduction

Lepton flavor violation (LFV) has been searched in several experiments. The current status in μ and τ decays is

$$\begin{aligned}\text{BR}(\mu \rightarrow e\gamma) &< 1.2 \times 10^{-11} \quad [1], \\ \text{BR}(\tau \rightarrow e\gamma) &< 2.7 \times 10^{-6} \quad [2], \\ \text{BR}(\tau \rightarrow \mu\gamma) &< 1.1 \times 10^{-6} \quad [3],\end{aligned}\tag{1}$$

and

$$\begin{aligned}\text{BR}(\mu \rightarrow 3e) &< 1.0 \times 10^{-12} \quad [4], \\ \text{BR}(\tau \rightarrow 3e) &< 2.9 \times 10^{-6} \quad [5], \\ \text{BR}(\tau \rightarrow 3\mu) &< 1.9 \times 10^{-6} \quad [5].\end{aligned}\tag{2}$$

In Z decays we have

$$\begin{aligned}\text{BR}(Z \rightarrow \mu e) &< 1.7 \times 10^{-6} \quad [6], \\ \text{BR}(Z \rightarrow \tau e) &< 9.8 \times 10^{-6} \quad [6], \\ \text{BR}(Z \rightarrow \tau\mu) &< 1.2 \times 10^{-5} \quad [7].\end{aligned}\tag{3}$$

These observations are obviously in agreement with the Standard Model (SM), where lepton flavor number is (perturbatively) conserved.

On the other hand, neutrino oscillations are a first evidence of LFV. Small neutrino masses and mixings of order one suggest the existence of a new scale around 10^{12} GeV [8]. Massive neutrinos could be naturally accommodated within the SM (the so called ν SM). The contributions from the light neutrino sector to other LFV processes, however, would be very small: $\text{BR}(\ell_J \rightarrow \ell_I \gamma) \lesssim 10^{-48}$ and $\text{BR}(Z \rightarrow \ell_I \ell_J) \lesssim 10^{-54}$ [9]. In consequence, any experimental signature of LFV in the charged sector would be a clear signature of nonstandard physics.

In this paper we will study the implications of supersymmetry (SUSY) on $Z \rightarrow \ell_I \ell_J$.¹ The GigaZ option of the TESLA Linear Collider project [11] could reduce the LEP bounds down to [12]

$$\begin{aligned}\text{BR}(Z \rightarrow \mu e) &< 2.0 \times 10^{-9} \\ \text{BR}(Z \rightarrow \tau e) &< \kappa \times 6.5 \times 10^{-8} \\ \text{BR}(Z \rightarrow \tau\mu) &< \kappa \times 2.2 \times 10^{-8},\end{aligned}\tag{4}$$

with $\kappa = 0.2 - 1.0$. We will here explore the possibility that SUSY provides a signal accessible to GigaZ in consistency with current bounds from $\text{BR}(\ell_J \rightarrow \ell_I \gamma)$. Note that in SUSY models the branching ratio $\text{BR}(\ell_J \rightarrow 3\ell_I) \approx \alpha_{em} \text{BR}(\ell_J \rightarrow \ell_I \gamma)$ will place weaker bounds on SUSY parameters (see Eqs. (1,2)) The conversion rate $\mu \rightarrow e$ on Ti gives also weaker bounds at current experiments, although this may change in the future (see [13] for a recent review).

¹A recent work on the flavor-changing decays $Z \rightarrow d_I d_J$ in 2HDM and SUSY has been presented in [10].

We will concentrate on the minimal SUSY extension of the SM (MSSM) with R-parity and general soft SUSY-breaking terms. Related works on LFV in Z decays in SUSY models study the MSSM [14] and a left-right SUSY model [15]. Several groups have analyzed other LFV processes in SUSY grand unified models with massive neutrinos (motivated by the atmospheric and solar neutrino anomalies [16]), or with R-parity violation [17]. There are also studies [18, 19] relating LFV Z decays with other processes. Direct signals of lepton flavour non-conservation in slepton production at the LHC [20] and at future e^+e^- or $\mu^+\mu^-$ colliders [21] have been also explored.

Other works on LFV Z decays in alternative models include the SM with massive Dirac or Majorana neutrinos [9], models with a heavy Z' boson [22], two Higgs doublet models (2HDMs) [23] or technicolor [24].

2 Calculation

The most general vertex $V\bar{\ell}_I\ell_J$ coupling a (lepton) fermion current to a vector boson can be parametrized in terms of four form factors:

$$\mathcal{M} = i\varepsilon_V^\mu \bar{u}_{\ell_I}(p_2) [\gamma_\mu(F_V - F_A\gamma_5) + (iF_M + F_E\gamma_5)\sigma_{\mu\nu}q^\nu] u_{\ell_J}(p_1), \quad (5)$$

where ε_V is the polarization vector ($\varepsilon_V \cdot q = 0$) and $q = p_2 - p_1$ is the momentum transfer. For an on-shell (massless) photon $F_A = 0$, and, in addition, if $m_I \neq m_J$ then $F_V = 0$. This implies that the flavor-changing process $\ell_J \rightarrow \ell_I\gamma$ is determined by (chirality flipping) dipole transitions only. In contrast, all form factors contribute to the decay of a Z boson:

$$\begin{aligned} \text{BR}(Z \rightarrow \ell_I\ell_J) &\equiv \text{BR}(Z \rightarrow \bar{\ell}_I\ell_J) + \text{BR}(Z \rightarrow \ell_I\bar{\ell}_J) \\ &= \frac{\alpha_W^3 M_Z}{48\pi^2 \Gamma_Z} \left[|f_L|^2 + |f_R|^2 + \frac{1}{c_W^2} (|f_M|^2 + |f_E|^2) \right], \end{aligned} \quad (6)$$

with $\alpha_W = g^2/(4\pi)$, $f_{L,R} = f_V \pm f_A$, $f_{V,A} \equiv -16\pi^2 g^{-3} F_{V,A}$ and $f_{M,E} \equiv -16M_W \pi^2 g^{-3} F_{M,E}$. We calculate (see Appendices A and B for details) these branching ratios in the MSSM.

Let us consider the case with two lepton families. Since SUSY is broken, fermion and scalar mass matrices will be diagonalized by different rotations in flavor space. After the diagonalization of the fermion sector we are left with a 2×2 scalar matrix with 3 arbitrary parameters. We will assume that the rotation that diagonalizes the scalar matrix is maximal, $\theta = \pi/4$ (i.e. we assume no alignment between fermion and scalar fields). We then parametrize [25] the two mass eigenvalues \tilde{m}_1^2 and \tilde{m}_2^2 in terms of $\tilde{m}^2 = \tilde{m}_1\tilde{m}_2$ and $\delta = (\tilde{m}_2^2 - \tilde{m}_1^2)/(2\tilde{m}^2)$:

$$\tilde{m}_{1,2}^2 = \tilde{m}^2 (\sqrt{1 + \delta^2} \mp \delta). \quad (7)$$

In this parametrization \tilde{m}^2 characterizes the SUSY-breaking scale and δ the mass splitting between the two families. δ is also responsible for any flavor-changing process: $\delta = 0$ corresponds to the flavor-conserving case, $\delta \ll 1$ can be treated as a non-diagonal mass insertion,

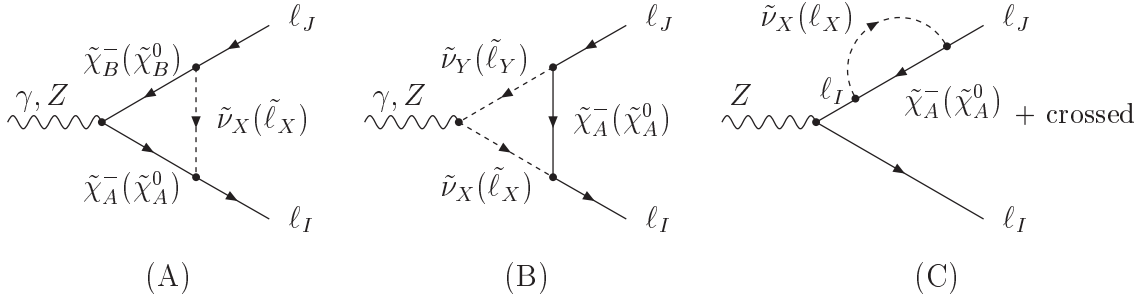


Figure 1: SUSY contributions to the LFV processes $Z \rightarrow \ell_I \ell_J$ and $\ell_J \rightarrow \ell_I \gamma$.

and $\delta \rightarrow \infty$ gives $\tilde{m}_2^2 \rightarrow \infty$ (a decoupled second family). The last case implies a maximum flavor-changing rate [14, 15].

In the analysis of $Z \rightarrow \ell_I \ell_J$ and $\ell_J \rightarrow \ell_I \gamma$ we will neglect the slepton mixing with a third family, which reduces the problem to the two family case above. The relevant parameters for the calculation will then be the masses and mixings of charginos and neutralinos; the masses and mixings of the four (‘left’ and ‘right’ handed) charged sleptons; and the masses and mixings of the two sneutrinos. In addition, we will separate the contribution of each δ^{IJ} by setting all the other to zero. Then, the mixing parameters in the sneutrino sector are just $\delta_{LL}^{\tilde{\nu} IJ}$, whereas for the charged sleptons we have $\delta_{LL}^{\tilde{\ell} IJ}$, $\delta_{RR}^{\tilde{\ell} IJ}$ and $\delta_{LR}^{\tilde{\ell} IJ}$.

In our analysis we will not assume any relation between slepton masses. For each non-zero choice of δ^{IJ} it is straightforward to obtain and diagonalize the mass matrix that corresponds to a maximal rotation angle (see Appendix B). Our results should coincide with the ones obtained in the limit of small mass difference using the mass insertion method, but they are also valid for any large value of δ^{IJ} .

The process $Z \rightarrow \ell_I \ell_J$ goes through the diagrams in Fig. 1. Analogous diagrams describe $\ell_J \rightarrow \ell_I \gamma$. The inclusion of the contributions of the third type is essential to cancel ultraviolet divergences (they are related to counterterms by Ward identities). Diagrams with neutralinos in (A) or sneutrinos in (B) do not couple to the photon. The diagrams of type (C) do not give dipole contributions.

Due to the weaker experimental bounds (in Table 1) on sneutrino masses, the dominant contributions to $Z \rightarrow \ell_I \ell_J$ will come from the diagrams mediated by chargino-sneutrino (see Fig. 2). Note that sneutrino masses can be substantially lighter than charged slepton masses for large $\tan \beta$ and light SUSY-breaking masses,

$$\begin{aligned}
 m_{\tilde{\nu}}^2 &\approx m_L^2 + \frac{1}{2} M_Z^2 \cos 2\beta, \\
 m_{\tilde{\ell}_L}^2 &\approx m_L^2 + \left(-\frac{1}{2} + s_W^2 \right) M_Z^2 \cos 2\beta,
 \end{aligned} \tag{8}$$

which tends to increase the maximum relative contribution of chargino-sneutrino diagrams.

We would like to emphasize that our results will depend on contributions with opposite

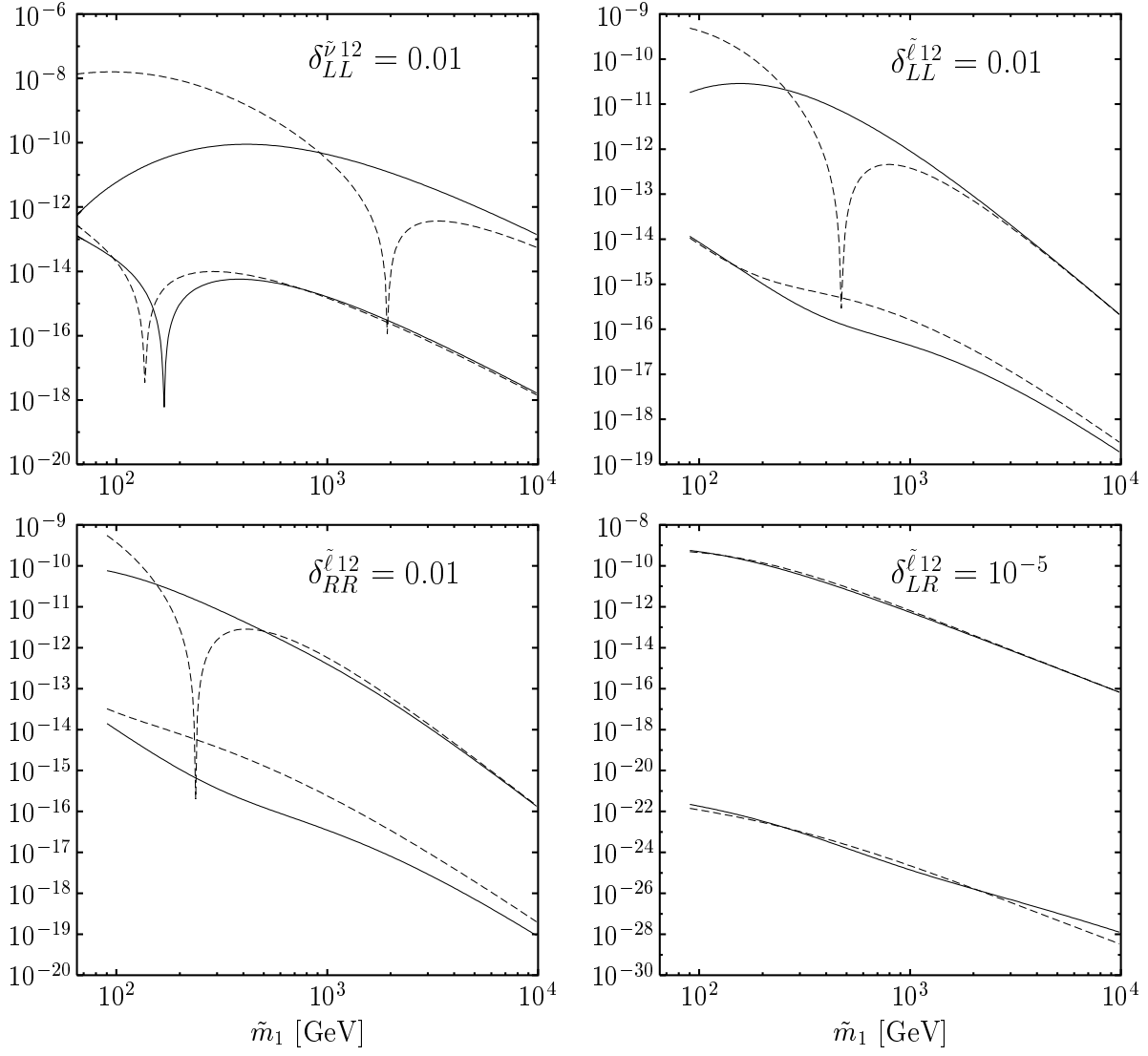


Figure 2: $\text{BR}(Z \rightarrow \mu e)$ (lower curves) and $\text{BR}(\mu \rightarrow e \gamma)$ (upper curves) as a function of the lightest scalar mass \tilde{m}_1 for $\tan \beta = 2$ and the different δ^{12} . Solid lines correspond to $M_2 = 150$ GeV and $\mu = -500$ GeV and dashed lines to $M_2 = \mu = 150$ GeV.

Table 1: Approximate lower bounds on SUSY mass parameters based on [26]. Note that, for negligible scalar trilinears, $m_{\tilde{\nu}}^2 = m_{\tilde{\ell}_L}^2 + M_Z^2 c_W^2 \cos 2\beta$, and the bounds on $m_{\tilde{\nu}}$ and $m_{\tilde{\ell}_L}$ are correlated. For instance: $m_{\tilde{\nu}} > 65$ (40) GeV for $\tan \beta = 2$ (50).

lightest slepton (\tilde{m}_1)	$m_{\tilde{\nu}} \geq 45$ GeV $m_{\tilde{\ell}_{L,R}} \geq 90$ GeV
lightest chargino	$m_{\tilde{\chi}_1^+} \geq 75$ GeV, if $m_{\tilde{\nu}} > m_{\tilde{\chi}_1^+}$ $m_{\tilde{\chi}_1^+} \geq 45$ GeV, otherwise
lightest neutralino	$m_{\tilde{\chi}_1^0} \geq 35$ GeV

signs that often cancel when varying a parameter. For example, one would expect that the process $Z \rightarrow \ell_I \ell_J$ is optimized for light slepton masses. However, we observe frequently the opposite effect. Its branching ratio can increase by raising the mass of the sleptons up to values of 500 GeV, and only at masses above 1 – 2 TeV the asymptotic regime is reached (see Fig. 2). These cancellations give a one or two orders of magnitude uncertainty to any naive estimate, and underline the need for a complete calculation like the one presented here.

We give in Fig. 3 the dominant diagrams in terms of gauginos, current eigenstates and mass insertions, specifying the chirality of the external fermion. All the diagrams contributing to $\ell_J \rightarrow \ell_I \gamma$ except for the last one grow with $\tan \beta$.

3 Results

3.1 $Z \rightarrow \ell_I \ell_J$ at TESLA GigaZ

Let us consider the process $Z \rightarrow \ell_I \ell_J$ uncorrelated from other LFV processes. For SUSY masses above the current limits it is possible to have $Z \rightarrow \mu e; \tau e; \tau \mu$ at the reach of GigaZ. The maximum rate is obtained when the second slepton $\tilde{\ell}_J$ is very heavy (i.e. $\delta^{IJ} \rightarrow \infty$). The largest contribution comes from virtual sneutrino–chargino diagrams (all other contributions are at least one order of magnitude smaller). It gives $\text{BR}(Z \rightarrow \ell_I \ell_J)$ from 2.5×10^{-8} for $\tan \beta = 2$ to 7.5×10^{-8} for $\tan \beta = 50$, practically independent of the lepton masses. The variation is due to the mild dependence of chargino and sneutrino masses on $\tan \beta$. These branching ratios are above the values given in Eq. (4). We find that a branching ratio larger than 2×10^{-9} (2×10^{-8}) can be obtained with sneutrino masses of up to 305 GeV (85 GeV) and chargino masses of up to 270 GeV (105 GeV).

Most of these values of $\text{BR}(Z \rightarrow \ell_I \ell_J)$, however, are correlated with an experimentally excluded rate of $\ell_J \rightarrow \ell_I \gamma$. In particular, after scanning for all the parameters in the model we find that $\text{BR}(\mu \rightarrow e \gamma) < 1.2 \times 10^{-11}$ implies $\text{BR}(Z \rightarrow \mu e) < 1.5 \times 10^{-10}$, which is below the

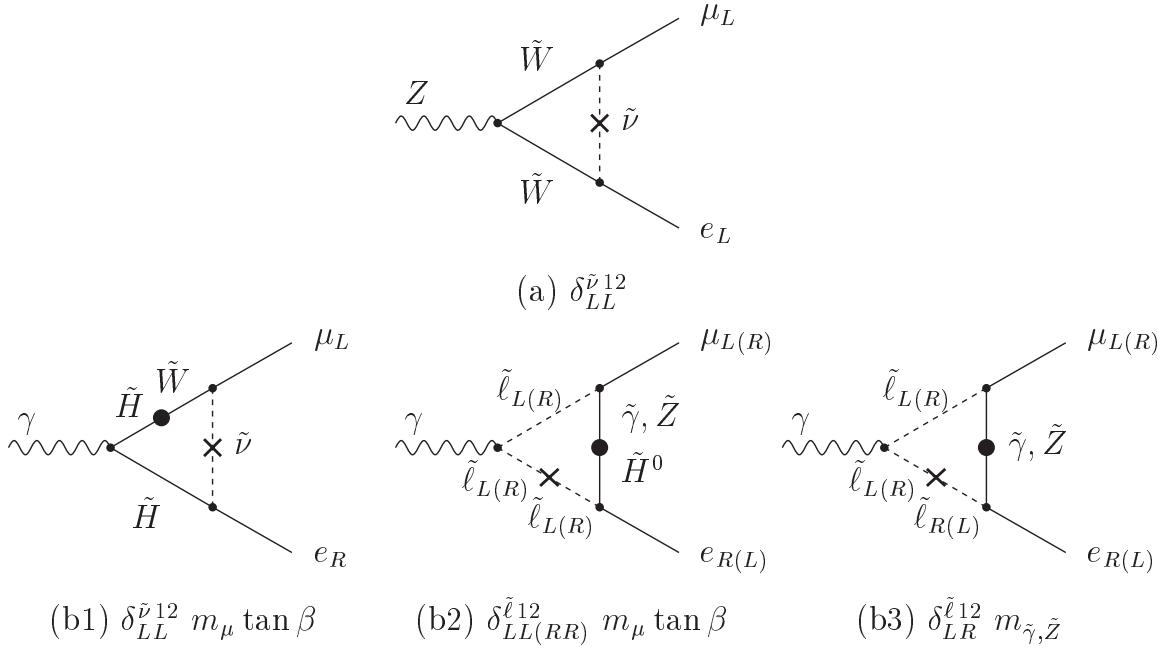


Figure 3: Dominant diagrams contributing to (a) $Z \rightarrow \mu e$ and (b) $\mu \rightarrow e \gamma$, in terms of gauginos, higgsinos and current eigenstates, showing the approximate linear dependence on the flavor-changing mass insertions δ^{12} (crosses), the fermion mass insertions (big dots) and $\tan \beta$.

reach of GigaZ.

A more promising result is obtained for the processes involving the τ lepton. It turns out (see also next Section) that the bounds from $\tau \rightarrow e \gamma; \mu \gamma$ can be avoided while still keeping a rate of $Z \rightarrow \tau e; \tau \mu$ at the reach of the best GigaZ projection (see Fig. 4). In particular, for large $\delta_{LL}^{\tilde{\nu}13,23}$ and a light sneutrino (of around 70 GeV) we get $\text{BR}(Z \rightarrow \tau e) \approx \text{BR}(Z \rightarrow \tau \mu) \approx 1.6 \times 10^{-8}$ for $\text{BR}(\tau \rightarrow e \gamma) \approx \text{BR}(\tau \rightarrow \mu \gamma) \approx 3.5 \times 10^{-8}$ (two orders of magnitude below current limits!). This result is due to the sneutrino-chargino diagram. The contributions due to charged slepton mixing are essentially different in the sense that they saturate the experimental bound to $\tau \rightarrow e \gamma; \mu \gamma$ giving a small effect (at most, one order of magnitude below the reach of GigaZ) in $Z \rightarrow \tau e; \tau \mu$. We obtain events at the reach of GigaZ with lightest sneutrino masses from 55 to 215 GeV, lightest chargino from 75 to 100 GeV, and $\tan \beta$ up to 7.

3.2 Bounds on δ^{IJ} from $\ell_J \rightarrow \ell_I \gamma$

The bounds on the mass insertions δ^{IJ} establish how severe is the flavor problem in the lepton sector of the MSSM. We will update them here, including in our work the calculation of the sneutrino-chargino contributions neglected in previous works [25].

The limits come exclusively from the process $\ell_J \rightarrow \ell_I \gamma$. To estimate the MSSM prediction we combine low and high values of the relevant parameters: $\tan \beta = 2; 50$, $m_{\tilde{\ell}} = 100; 500$ GeV,

Table 2: Bounds on the δ^{12} s from $\text{BR}(\mu \rightarrow e\gamma) < 1.2 \times 10^{-11}$ in different SUSY scenarios.

$\delta_{LL}^{\nu 12}$	\tilde{m}_1	M_2	$\mu = -500$	$\mu = -150$	$\mu = 150$	$\mu = 500$
$\tan \beta = 2$	100	150	14×10^{-3}	1.0×10^{-3}	0.3×10^{-3}	1.0×10^{-3}
		500	33×10^{-3}	3.0×10^{-3}	1.7×10^{-3}	13×10^{-3}
	500	150	3.7×10^{-3}	1.1×10^{-3}	1.2×10^{-3}	1.7×10^{-3}
		500	7.3×10^{-3}	2.6×10^{-3}	2.3×10^{-3}	4.1×10^{-3}
$\tan \beta = 50$	100	150	9.3×10^{-5}	2.1×10^{-5}	2.0×10^{-5}	8.6×10^{-5}
		500	80×10^{-5}	9.0×10^{-5}	8.8×10^{-5}	77×10^{-5}
	500	150	9.7×10^{-5}	4.5×10^{-5}	4.5×10^{-5}	9.4×10^{-5}
		500	22×10^{-5}	9.6×10^{-5}	9.5×10^{-5}	21×10^{-5}
$\delta_{LL}^{\ell 12}$	\tilde{m}_1	M_2	$\mu = -500$	$\mu = -150$	$\mu = 150$	$\mu = 500$
$\tan \beta = 2$	100	150	7.5×10^{-3}	2.6×10^{-3}	1.7×10^{-3}	5.0×10^{-3}
		500	84×10^{-3}	11×10^{-3}	7.0×10^{-3}	41×10^{-3}
	500	150	14×10^{-3}	8.5×10^{-3}	0.12	32×10^{-3}
		500	24×10^{-3}	20×10^{-3}	32×10^{-3}	26×10^{-3}
$\tan \beta = 50$	100	150	2.4×10^{-4}	0.8×10^{-4}	0.8×10^{-4}	2.4×10^{-4}
		500	24×10^{-4}	3.5×10^{-4}	3.4×10^{-4}	23×10^{-4}
	500	150	7.4×10^{-4}	6.4×10^{-4}	6.9×10^{-4}	7.6×10^{-4}
		500	9.7×10^{-4}	9.6×10^{-4}	9.8×10^{-4}	9.7×10^{-4}
$\delta_{RR}^{\ell 12}$	\tilde{m}_1	M_2	$\mu = -500$	$\mu = -150$	$\mu = 150$	$\mu = 500$
$\tan \beta = 2$	100	150	4.2×10^{-3}	1.5×10^{-3}	1.8×10^{-3}	3.7×10^{-3}
		500	11×10^{-3}	3.2×10^{-3}	2.5×10^{-3}	8.3×10^{-3}
	500	150	22×10^{-3}	10×10^{-3}	22×10^{-3}	0.33
		500	19×10^{-3}	12×10^{-3}	0.33	35×10^{-3}
$\tan \beta = 50$	100	150	1.6×10^{-4}	0.6×10^{-4}	0.6×10^{-4}	1.5×10^{-4}
		500	3.8×10^{-4}	1.1×10^{-4}	1.1×10^{-4}	3.8×10^{-4}
	500	150	16×10^{-4}	13×10^{-4}	15×10^{-4}	17×10^{-4}
		500	9.4×10^{-4}	8.1×10^{-4}	8.7×10^{-4}	9.6×10^{-4}
$\delta_{LR}^{\ell 12}$	\tilde{m}_1	M_2	$\mu = -500$	$\mu = -150$	$\mu = 150$	$\mu = 500$
$\tan \beta = 2$	100	150	1.6×10^{-6}	1.5×10^{-6}	1.6×10^{-6}	1.7×10^{-6}
		500	4.5×10^{-6}	4.4×10^{-6}	4.7×10^{-6}	4.6×10^{-6}
	500	150	1.3×10^{-6}	1.2×10^{-6}	1.2×10^{-6}	1.2×10^{-6}
		500	7.6×10^{-6}	7.5×10^{-6}	7.6×10^{-6}	7.7×10^{-6}
$\tan \beta = 50$	100	150	1.6×10^{-6}	1.5×10^{-6}	1.6×10^{-6}	1.6×10^{-6}
		500	4.5×10^{-6}	4.5×10^{-6}	4.6×10^{-6}	4.5×10^{-6}
	500	150	1.3×10^{-6}	1.2×10^{-6}	1.2×10^{-6}	1.3×10^{-6}
		500	7.7×10^{-6}	7.6×10^{-6}	7.6×10^{-6}	7.7×10^{-6}

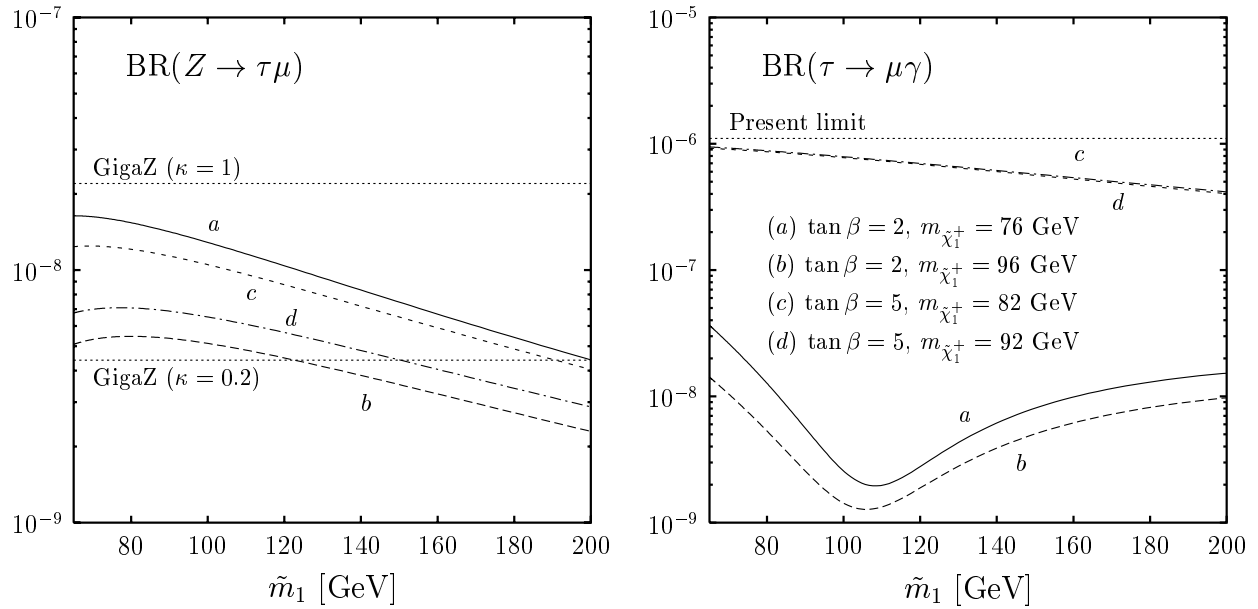


Figure 4: $\text{BR}(Z \rightarrow \tau\mu)$ and $\text{BR}(\tau \rightarrow \mu\gamma)$ as a function of the lightest sneutrino mass (\tilde{m}_1) with the other one decoupled ($\delta_{LL}^{\tilde{\nu}23} \rightarrow \infty$), in several SUSY scenarios at the reach of GigaZ.

and the gaugino and higgsino mass parameters $M_2 = 150; 500$ GeV and $\mu = \pm 150; \pm 500$ GeV.

In Table 2 we include the bounds from $\mu \rightarrow e\gamma$ to $\delta_{LL}^{\tilde{\nu}12}$, $\delta_{LL}^{\tilde{\ell}12}$, $\delta_{RR}^{\tilde{\ell}12}$ and $\delta_{LR}^{\tilde{\ell}12}$. A $\delta \approx 10^{-4}$ implies a 1% degeneracy between the two slepton masses. We observe that the degeneracy between the selectron and the smuon is required even for large SUSY masses, and it must be stronger if $\tan\beta$ is large, as expected from the diagrams in Fig. 3. The small values of $\delta_{LR}^{\tilde{\ell}12}$, around 10^{-6} , imply just that the scalar trilinears, usually assumed proportional to the Yukawa couplings, are small. Particularly weak bounds on the δ 's (bold faced in Table 2) are obtained when approaching a dip of the curves in Fig. 2. This occurs for certain values of the SUSY parameters due to cancellations of the contributions of the various particles running in the loops.

The experimental bounds on the mass insertions involving the third family are much weaker. In particular, for small $\tan\beta$ we find no bounds on any δ^{I3} (except for $\delta_{LR}^{\tilde{\ell}I3}$). For large $\tan\beta$ the bounds are (depending on the values of the SUSY-breaking masses) $\delta_{LL}^{\tilde{\nu}I3} = 0.03$ to 1.3 ; $\delta_{LL}^{\tilde{\ell}I3} = 0.14$ to ∞ ; and $\delta_{RR}^{\tilde{\ell}I3} = 0.11$ to ∞ . For the LR mass insertions we find $\delta_{LR}^{\tilde{\ell}I3} = 0.05$ to ∞ , independent of $\tan\beta$.

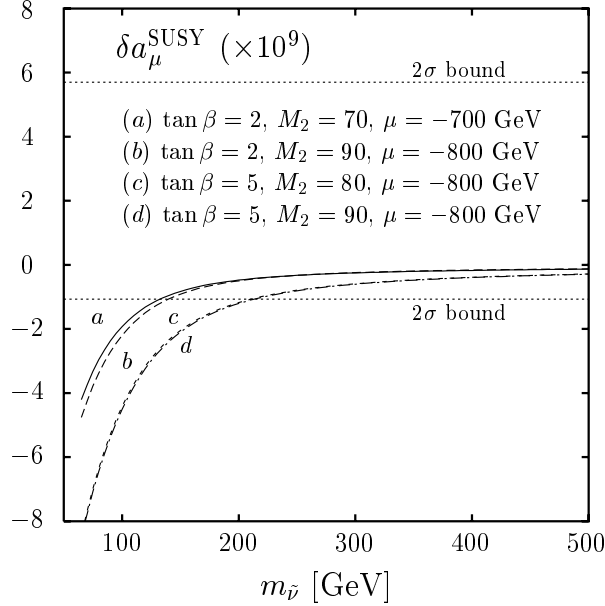


Figure 5: Total SUSY contribution to the muon anomalous magnetic dipole moment as a function of the sneutrino mass with $m_L = m_R$, in the same SUSY scenarios as in Fig. 4.

3.3 Lepton flavor violation and $g_\mu - 2$

Finally we would like to comment on the relation between $\mu \rightarrow e\gamma$ and the muon anomalous magnetic dipole moment.² A $g_\mu - 2$ correction would be generated by the diagrams in Fig. 3b if no mass insertions $\delta_{LL}^{\tilde{\nu}IJ}$ or $\delta_{RR}^{\tilde{\nu}IJ}$ are included or $\delta_{LR}^{\tilde{\nu}IJ}$ is replaced by $\delta_{LR}^{\tilde{\ell}22}$. In this sense, $g_\mu - 2$ is a normalization of the branching ratio $\text{BR}(\ell_J \rightarrow \ell_I \gamma)$ for processes changing the muon flavor.

We plot in Fig. 5 the value of $a_\mu = (g_\mu - 2)/2$ for the SUSY parameters in the region accessible to GigaZ not excluded by $\tau \rightarrow \mu\gamma$, taking for simplicity equal soft-breaking terms $m_L = m_R$ (they would not very different, for example, assuming left-right unification at the GUT scale). We obtain, in agreement with [28], positive or negative contributions correlated with the sign of the Higgsino mass parameter μ and similar in size to the weak corrections. The recently revised SM prediction [29], $a_\mu^{\text{SM}} = 11\,659\,179.2\,(9.4) \times 10^{-10}$, compared to the world average after the last data from the Brookhaven E821 experiment [30], $a_\mu^{\text{exp}} = 11\,659\,202.3\,(15.1) \times 10^{-10}$, exhibits a 1.4σ discrepancy: $\delta a_\mu = a_\mu^{\text{exp}} - a_\mu^{\text{SM}} = (23.1 \pm 16.9) \times 10^{-10}$. This indicates that the muon dipole moment may still need non-standard contributions of positive sign. In any case, the MSSM contribution $\delta a_\mu^{\text{SUSY}}$ is bounded at two standard deviations by the dotted lines in Fig. 5. Only the regions with heavier masses in the scenarios of Fig. 4 are favored.

Fig. 6 shows the muon anomalous magnetic moment for the different sets of SUSY parameters employed to explore the muon LFV decay in Table 2. Low values of $\tan\beta$ and positive

²See [27] for more exhaustive analyses of the constraints on lepton flavor violation in the MSSM from the muon anomalous magnetic moment measurement.

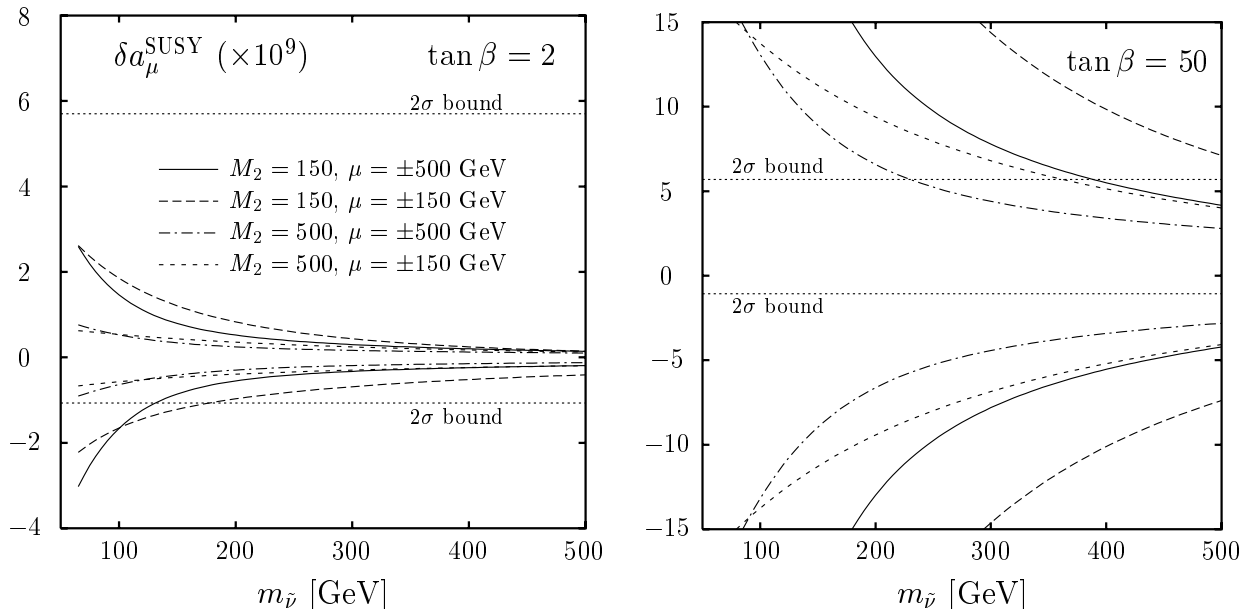


Figure 6: Total SUSY contribution to the muon anomalous magnetic dipole moment as a function of the sneutrino mass, with $m_L = m_R$.

values of μ are preferred by $g_\mu - 2$, which implies less stringent bounds on the δ insertions parametrizing the flavor-changing lepton decays.

4 Conclusions

SUSY models introduce LFV corrections which are proportional to slepton mass squared differences. We have shown that the non-observation of $\mu \rightarrow e\gamma$ implies around a 5% degeneracy between the masses of the sleptons in the first two families. Moreover, once this degeneracy is imposed, the rate of $Z \rightarrow \mu e$ is below the limits to be explored at GigaZ. The degeneracy between the lightest slepton families could be justified by the weakness of its Yukawa couplings, but this would not be the case for the third family.

We have shown that the current bounds on $\tau \rightarrow e\gamma; \mu\gamma$ introduce only weak constraints on the SUSY-breaking parameters: there is no flavor problem for the third lepton family. If the GigaZ option of TESLA reaches its best projected sensitivity, it could observe $Z \rightarrow \tau e; \tau\mu$ coming from the virtual exchange of wino-sneutrino.

Acknowledgments. JII acknowledges the Theory Group of DESY Zeuthen and MM the Institute for Nuclear Research (Moscow) for their kind hospitality. We thank F. del Aguila, J. Prades and T. Riemann for useful discussions. This work has been supported by CICYT, Junta de Andalucía and the European Union under contracts FPA2000-1558, FQM-101 and HPRN-CT-2000-00149, respectively.

A Generic expressions at one loop for $Z\bar{\ell}_I\ell_J$

A.1 Feynman rules in terms of generic vertex couplings

Let f be a fermion, ϕ a scalar field and $P_{R,L} = (1 \pm \gamma_5)/2$. The Feynman rules for the three vertex topologies needed are:

- Vertex $Z\bar{f}_A f_B$: $ig\gamma^\mu(g_{AB}^L P_L + g_{AB}^R P_R)$,
- Vertex $Z\phi_X^\dagger(p_2)\phi_Y(p_1)$: $igG_{XY}(p_1 + p_2)^\mu$,
- Vertex $\phi_X^\dagger \bar{f}_A f_I$: $ig(c_{IAX}^L P_L + c_{IAX}^R P_R)$.

A.2 Invariant amplitude

The most general invariant amplitude for on-shell external legs is

$$\mathcal{M} = -ig \frac{\alpha_W}{4\pi} \varepsilon_Z^\mu \bar{u}_{\ell_I}(p_2) \left[\gamma_\mu (f_V - f_A \gamma_5) + \frac{\sigma_{\mu\nu} q^\nu}{M_W} (if_M + f_E \gamma_5) \right] u_{\ell_J}(p_1). \quad (9)$$

Let us introduce the squared mass ratios $\lambda_n = m_n^2/M_W^2$ and the dimensionless two- and three-point one-loop integrals

$$\mathbb{B}_1(\lambda_0, \lambda_1) \equiv B_1(0; m_0^2, m_1^2), \quad (10)$$

$$\mathbb{C}_..(\lambda_0, \lambda_1, \lambda_2) \equiv M_W^2 C_{..}(0, M_Z^2, 0; m_0^2, m_1^2, m_2^2), \quad (11)$$

from the usual tensor integrals [31, 32],

$$B^\mu(p^2; m_0^2, m_1^2) = p^\mu B_1, \quad (12)$$

$$C^\mu(p_1^2, Q^2, p_2^2; m_0^2, m_1^2, m_2^2) = p_1^\mu C_{11} + p_2^\mu C_{12}, \quad (13)$$

$$C^{\mu\nu}(p_1^2, Q^2, p_2^2; m_0^2, m_1^2, m_2^2) = p_1^\mu p_1^\nu C_{21} + p_2^\mu p_2^\nu C_{22} + (p_1^\mu p_2^\nu + p_2^\mu p_1^\nu) C_{23} + g^{\mu\nu} M_W^2 C_{24}. \quad (14)$$

Note that \mathbb{C}_0 , \mathbb{C}_{23} , \mathbb{C}_{24} , $\mathbb{C}_{11} + \mathbb{C}_{12}$ and $\mathbb{C}_{21} + \mathbb{C}_{22}$ are symmetric under the replacements $\lambda_1 \leftrightarrow \lambda_2$, while $\mathbb{C}_{11} - \mathbb{C}_{12}$ and $\mathbb{C}_{21} - \mathbb{C}_{22}$ are antisymmetric. The form factors for each type of diagrams (Fig. 1) are:

- Diagram of type A:

$$f_L^{\chi\chi s} = \sum_{XAB} \left\{ g_{AB}^L c_{IAX}^{L*} c_{JBX}^L \sqrt{\lambda_A \lambda_B} \mathbb{C}_0(\lambda_X, \lambda_A, \lambda_B) + g_{AB}^R c_{IAX}^{L*} c_{JBX}^L \left[\lambda_Z \mathbb{C}_{23}(\lambda_X, \lambda_A, \lambda_B) - 2 \mathbb{C}_{24}(\lambda_X, \lambda_A, \lambda_B) + \frac{1}{2} \right] \right\}, \quad (15)$$

$$f_R^{\chi\chi s} = f_L^{\chi\chi s} (L \leftrightarrow R), \quad (16)$$

$$f_M^{\chi\chi^s} = \sum_{XAB} \left\{ \frac{\sqrt{\lambda_J}}{2} [(g_{AB}^R c_{IAX}^{L*} c_{JBX}^L + g_{AB}^L c_{IAX}^{R*} c_{JBX}^R) + (I \leftrightarrow J)^*] \right. \\ \times [\mathbb{C}_{11}(\lambda_X, \lambda_A, \lambda_B) + \mathbb{C}_{21}(\lambda_X, \lambda_A, \lambda_B) + \mathbb{C}_{23}(\lambda_X, \lambda_A, \lambda_B)] \\ \left. + \frac{\sqrt{\lambda_A}}{2} [(g_{AB}^L c_{IAX}^{L*} c_{JBX}^R + g_{AB}^R c_{IAX}^{R*} c_{JBX}^L) + (I \leftrightarrow J)^*] \mathbb{C}_{12}(\lambda_X, \lambda_A, \lambda_B) \right\}, \quad (17)$$

$$if_E^{\chi\chi^s} = \sum_{XAB} \left\{ \frac{\sqrt{\lambda_J}}{2} [(g_{AB}^R c_{IAX}^{L*} c_{JBX}^L - g_{AB}^L c_{IAX}^{R*} c_{JBX}^R) - (I \leftrightarrow J)^*] \right. \\ \times [\mathbb{C}_{11}(\lambda_X, \lambda_A, \lambda_B) + \mathbb{C}_{21}(\lambda_X, \lambda_A, \lambda_B) + \mathbb{C}_{23}(\lambda_X, \lambda_A, \lambda_B)] \\ \left. + \frac{\sqrt{\lambda_A}}{2} [(g_{AB}^L c_{IAX}^{L*} c_{JBX}^R - g_{AB}^R c_{IAX}^{R*} c_{JBX}^L) - (I \leftrightarrow J)^*] \mathbb{C}_{12}(\lambda_X, \lambda_A, \lambda_B) \right\}. \quad (18)$$

• Diagram of type B:

$$f_L^{ss\chi} = -2 \sum_{AXY} G_{XY} c_{IAX}^{L*} c_{JAY}^L \mathbb{C}_{24}(\lambda_A, \lambda_X, \lambda_Y), \quad (19)$$

$$f_R^{ss\chi} = f_L^{ss\chi} (L \leftrightarrow R), \quad (20)$$

$$f_M^{ss\chi} = \sum_{AXY} \left\{ -\frac{\sqrt{\lambda_J}}{2} [G_{XY} (c_{IAX}^{L*} c_{JAY}^L + c_{IAX}^{R*} c_{JAY}^R) + (I \leftrightarrow J)^*] \right. \\ \times [\mathbb{C}_{11}(\lambda_A, \lambda_X, \lambda_Y) + \mathbb{C}_{12}(\lambda_A, \lambda_X, \lambda_Y) + \mathbb{C}_{23}(\lambda_A, \lambda_X, \lambda_Y)] \\ \left. + \frac{\sqrt{\lambda_A}}{2} [G_{XY} c_{IAX}^{L*} c_{JAY}^R + (I \leftrightarrow J)^*] \right. \\ \left. \times [\mathbb{C}_0(\lambda_A, \lambda_X, \lambda_Y) + \mathbb{C}_{11}(\lambda_A, \lambda_X, \lambda_Y) + \mathbb{C}_{12}(\lambda_A, \lambda_X, \lambda_Y)] \right\}, \quad (21)$$

$$if_E^{ss\chi} = \sum_{AXY} \left\{ -\frac{\sqrt{\lambda_J}}{2} [G_{XY} (c_{IAX}^{L*} c_{JAY}^L - c_{IAX}^{R*} c_{JAY}^R) - (I \leftrightarrow J)^*] \right. \\ \times [\mathbb{C}_{11}(\lambda_A, \lambda_X, \lambda_Y) + \mathbb{C}_{12}(\lambda_A, \lambda_X, \lambda_Y) + \mathbb{C}_{23}(\lambda_A, \lambda_X, \lambda_Y)] \\ \left. + \frac{\sqrt{\lambda_A}}{2} [G_{XY} c_{IAX}^{L*} c_{JAY}^R - (I \leftrightarrow J)^*] \right. \\ \left. \times [\mathbb{C}_0(\lambda_A, \lambda_X, \lambda_Y) + \mathbb{C}_{11}(\lambda_A, \lambda_X, \lambda_Y) + \mathbb{C}_{12}(\lambda_A, \lambda_X, \lambda_Y)] \right\}. \quad (22)$$

• Diagram of type C:

$$f_L^{\chi^s} = -\frac{\cos 2\theta_W}{2c_W} \sum_{AX} c_{IAX}^{L*} c_{JAX}^L \mathbb{B}_1(\lambda_A, \lambda_X), \quad (23)$$

$$f_R^{\chi^s} = \frac{s_W^2}{c_W} \sum_{AX} c_{IAX}^{R*} c_{JAX}^R \mathbb{B}_1(\lambda_A, \lambda_X), \quad (24)$$

$$f_M^{\chi^s} = 0, \quad (25)$$

$$f_E^{\chi^s} = 0. \quad (26)$$

The tensor integrals are numerically evaluated with the computer program `LoopTools` [33], based on `FF` [34].

Non-trivial checks of our expressions are the finiteness of the amplitude and the test of the decoupling of heavy particles running in the loops, that must take place both in the SM and the MSSM [35]. These conditions are fulfilled only when summing over the different type of diagrams involved thanks to the relations existing among vertex couplings. Note that the ultraviolet-divergent tensor integrals are the same that diverge with a large mass M ,

$$\mathbb{C}_{24} \rightarrow -\frac{1}{2\epsilon} - \frac{1}{2} \log M, \quad \mathbb{B}_1 \rightarrow \frac{1}{\epsilon} + \log M, \quad \epsilon = D - 4. \quad (27)$$

All the other tensor integrals are finite and vanish for large masses.

B Masses, mixings and vertex couplings in the MSSM

Notation: the indices I or J refer to the flavor of the external fermion; the indices A or B refer to a chargino/neutralino mass eigenstate ($\tilde{\chi}_{A=1,2}^{\pm}$ and $\tilde{\chi}_{A=1,2,3,4}^0$); the indices X or Y refer to a charged slepton/sneutrino mass eigenstate ($\tilde{\ell}_{X=1,\dots,6}$ and $\tilde{\nu}_{X=1,2,3}$).

B.1 Charged sleptons

Let $\tilde{\ell}_{L_I}$ and $\tilde{\ell}_{R_I}$ be the superpartners of the charged leptons ℓ_{L_I} and ℓ_{R_I} , respectively. The 6×6 mass matrix of three generations of (charged) sleptons can be written as

$$\mathbf{M}_{\tilde{\ell}}^2 = \begin{pmatrix} \mathbf{m}_{LL}^2 & \mathbf{m}_{LR}^2{}^T \\ \mathbf{m}_{LR}^2 & \mathbf{m}_{RR}^2 \end{pmatrix} \quad (28)$$

where \mathbf{m}_{LL}^2 and \mathbf{m}_{RR}^2 are 3×3 hermitian matrices and \mathbf{m}_{LR}^2 is a 3×3 matrix, given by

$$(\mathbf{m}_{LL}^2)_{IJ} = (\mathbf{m}_L^2)_{IJ} + \left[m_{\ell_I}^2 + \left(-\frac{1}{2} + s_W^2 \right) M_Z^2 \cos 2\beta \right] \delta_{IJ}, \quad (29)$$

$$(\mathbf{m}_{RR}^2)_{IJ} = (\mathbf{m}_R^2)_{IJ} + [m_{\ell_I}^2 - M_Z^2 \cos 2\beta s_W^2] \delta_{IJ}, \quad (30)$$

$$(\mathbf{m}_{LR}^2)_{IJ} = (\mathbf{A}_{\ell})_{IJ} \frac{v \cos \beta}{\sqrt{2}} - m_{\ell_I} \mu \tan \beta \delta_{IJ}. \quad (31)$$

The mass matrix $\mathbf{M}_{\tilde{\ell}}^2$ can be diagonalized by a 6×6 unitary matrix $\mathbf{S}^{\tilde{\ell}}$,

$$\mathbf{S}^{\tilde{\ell}} \mathbf{M}_{\tilde{\ell}}^2 \mathbf{S}^{\tilde{\ell}\dagger} = \mathbf{diag}(m_{\tilde{\ell}_X}^2), \quad X = 1, \dots, 6. \quad (32)$$

The mass eigenstates are then given by

$$\tilde{\ell}_X = \mathbf{S}_{X,I}^{\tilde{\ell}} \tilde{\ell}_{L_I} + \mathbf{S}_{X,I+3}^{\tilde{\ell}} \tilde{\ell}_{R_I}, \quad X = 1, \dots, 6, \quad I = 1, 2, 3. \quad (33)$$

B.2 Sneutrinos

There are only ‘left-handed’ sneutrinos in the MSSM. Let $\tilde{\nu}_{L_I}$ be the superpartner of the left-handed neutrino ν_I . Then the 3×3 sneutrino mass matrix contains the same soft SUSY-breaking mass term as the ‘left-handed’ sleptons and a different D term:

$$(\mathbf{M}_{\tilde{\nu}}^2)_{IJ} = (\mathbf{m}_{\tilde{L}}^2)_{IJ} + \frac{1}{2}M_Z^2 \cos 2\beta \delta_{IJ}, \quad (34)$$

and it is diagonalized by a 3×3 unitary matrix $\mathbf{S}^{\tilde{\nu}}$,

$$\mathbf{S}^{\tilde{\nu}} \mathbf{M}_{\tilde{\nu}}^2 \mathbf{S}^{\tilde{\nu}\dagger} = \mathbf{diag}(m_{\tilde{\nu}_X}^2), \quad X = 1, 2, 3, \quad (35)$$

so that the sneutrino mass eigenstates are

$$\tilde{\nu}_X = \mathbf{S}_{X,I}^{\tilde{\nu}} \tilde{\nu}_{L_I}, \quad X = 1, 2, 3, \quad I = 1, 2, 3. \quad (36)$$

B.3 Slepton matrices in terms of δ mass insertions

Assuming that only two generations (I and J) of charged sleptons mix and they do it maximally ($\theta = \pi/4$), only the following 4×4 symmetric mass matrix, with entries $I, J, I+3, J+3$, is relevant:

$$\mathbf{M}_{\tilde{\ell}}^2 = \tilde{m}^2 \begin{pmatrix} 1 & \cdot & \cdot & \cdot \\ \delta_{LL}^{\tilde{\ell} IJ} & 1 & \cdot & \cdot \\ \delta_{LR}^{\tilde{\ell} II} & \delta_{LR}^{\tilde{\ell} IJ} & 1 & \cdot \\ \delta_{LR}^{\tilde{\ell} JI} & \delta_{LR}^{\tilde{\ell} JJ} & \delta_{RR}^{\tilde{\ell} IJ} & 1 \end{pmatrix}. \quad (37)$$

We assume that only one of these δ ’s is different from zero. Then, the 4×4 unitary matrix $\mathbf{S}^{\tilde{\ell}}$ diagonalizing $\mathbf{M}_{\tilde{\ell}}^2$ and the corresponding eigenvalues are, in each case:

$$\delta_{LL}^{\tilde{\ell} IJ} \equiv \delta \neq 0; \quad \mathbf{S}^{\tilde{\ell}} = \begin{pmatrix} \frac{1}{\sqrt{2}} & -\frac{1}{\sqrt{2}} & 0 & 0 \\ \frac{1}{\sqrt{2}} & \frac{1}{\sqrt{2}} & 0 & 0 \\ 0 & 0 & 1 & 0 \\ 0 & 0 & 0 & 1 \end{pmatrix}; \quad \begin{aligned} \tilde{m}_I^2 &= \tilde{m}^2(\sqrt{1+\delta^2} - \delta), \\ \tilde{m}_J^2 &= \tilde{m}^2(\sqrt{1+\delta^2} + \delta), \\ \tilde{m}_{I+3}^2 &= \tilde{m}^2, \\ \tilde{m}_{J+3}^2 &= \tilde{m}^2. \end{aligned} \quad (38)$$

$$\delta_{RR}^{\tilde{\ell} IJ} \equiv \delta \neq 0; \quad \mathbf{S}^{\tilde{\ell}} = \begin{pmatrix} 1 & 0 & 0 & 0 \\ 0 & 1 & 0 & 0 \\ 0 & 0 & \frac{1}{\sqrt{2}} & -\frac{1}{\sqrt{2}} \\ 0 & 0 & \frac{1}{\sqrt{2}} & \frac{1}{\sqrt{2}} \end{pmatrix}; \quad \begin{aligned} \tilde{m}_I^2 &= \tilde{m}^2, \\ \tilde{m}_J^2 &= \tilde{m}^2, \\ \tilde{m}_{I+3}^2 &= \tilde{m}^2(\sqrt{1+\delta^2} - \delta), \\ \tilde{m}_{J+3}^2 &= \tilde{m}^2(\sqrt{1+\delta^2} + \delta). \end{aligned} \quad (39)$$

$$\delta_{LR}^{\tilde{\ell} IJ} \equiv \delta \neq 0; \quad \mathbf{S}^{\tilde{\ell}} = \begin{pmatrix} \frac{1}{\sqrt{2}} & 0 & 0 & -\frac{1}{\sqrt{2}} \\ 0 & 1 & 0 & 0 \\ 0 & 0 & 1 & 0 \\ \frac{1}{\sqrt{2}} & 0 & 0 & \frac{1}{\sqrt{2}} \end{pmatrix}; \quad \begin{aligned} \tilde{m}_I^2 &= \tilde{m}^2(\sqrt{1+\delta^2} - \delta), \\ \tilde{m}_J^2 &= \tilde{m}^2, \\ \tilde{m}_{I+3}^2 &= \tilde{m}^2, \\ \tilde{m}_{J+3}^2 &= \tilde{m}^2(\sqrt{1+\delta^2} + \delta). \end{aligned} \quad (40)$$

$$\delta_{LR}^{\tilde{\ell} JJ} \equiv \delta \neq 0; \quad \mathbf{S}^{\tilde{\ell}} = \begin{pmatrix} 1 & 0 & 0 & 0 \\ 0 & \frac{1}{\sqrt{2}} & -\frac{1}{\sqrt{2}} & 0 \\ 0 & \frac{1}{\sqrt{2}} & \frac{1}{\sqrt{2}} & 0 \\ 0 & 0 & 0 & 1 \end{pmatrix}; \quad \begin{aligned} \tilde{m}_I^2 &= \tilde{m}^2, \\ \tilde{m}_J^2 &= \tilde{m}^2(\sqrt{1+\delta^2} - \delta), \\ \tilde{m}_{I+3}^2 &= \tilde{m}^2(\sqrt{1+\delta^2} + \delta), \\ \tilde{m}_{J+3}^2 &= \tilde{m}^2. \end{aligned} \quad (41)$$

The insertions $\delta_{LR}^{\tilde{\ell} II}$ and $\delta_{LR}^{\tilde{\ell} JJ}$ are flavor conserving. The 2×2 mixing matrix for the sneutrinos in terms of the mass insertion $\delta_{LL}^{\tilde{\nu} IJ}$ is constructed in a similar way.

B.4 Charginos

The chargino mass matrix, in the (charged wino, charged Higgsino) basis, is

$$\mathbf{X} = \begin{pmatrix} M_2 & \sqrt{2}M_W \sin \beta \\ \sqrt{2}M_W \cos \beta & \mu \end{pmatrix}. \quad (42)$$

It can be diagonalized by two unitary matrices \mathbf{U} and \mathbf{V} ,

$$\mathbf{U}^* \mathbf{X} \mathbf{V}^{-1} = \mathbf{diag}(m_{\tilde{\chi}_1^\pm}, m_{\tilde{\chi}_2^\pm}), \quad (43)$$

where

$$\begin{aligned} m_{\tilde{\chi}_{1,2}^\pm}^2 &= \frac{1}{2} \left[M_2^2 + \mu^2 + 2M_W^2 \right. \\ &\quad \left. \mp \sqrt{(M_2^2 - \mu^2)^2 + 4M_W^4 \cos^2 2\beta + 4M_W^2(M_2^2 + \mu^2 + 2M_2\mu \sin 2\beta)} \right]. \end{aligned} \quad (44)$$

In order to get positive-mass eigenstates, one introduces two orthogonal matrices \mathbf{O}_\pm ,

$$\mathbf{U} = \mathbf{O}_- \quad (45)$$

$$\mathbf{V} = \begin{cases} \mathbf{O}_+ & , \det \mathbf{X} > 0 \\ \sigma_3 \mathbf{O}_+ & , \det \mathbf{X} < 0 \end{cases} \quad (46)$$

where σ_3 is the usual Pauli matrix.

B.5 Neutralinos

The neutralino mass matrix, in the basis of the U(1) and SU(2) neutral gauginos and the two neutral Higgsinos ($\tilde{B}, \tilde{W}_3, \tilde{H}_1^0, \tilde{H}_2^0$), is the symmetric matrix:

$$\mathbf{Y} = \begin{pmatrix} M_1 & \cdot & \cdot & \cdot \\ 0 & M_2 & \cdot & \cdot \\ -M_Z s_W \cos \beta & M_Z c_W \cos \beta & 0 & \cdot \\ M_Z s_W \sin \beta & -M_Z c_W \sin \beta & -\mu & 0 \end{pmatrix}. \quad (47)$$

To simplify, we employ the unification constraint $M_1 = \frac{5}{3} \tan^2 \theta_W M_2$.

The matrix above can be numerically diagonalized by the unitary matrix \mathbf{N} ,

$$\mathbf{N}^* \mathbf{Y} \mathbf{N}^{-1} = \mathbf{diag}(m_{\tilde{\chi}_1^0}, m_{\tilde{\chi}_2^0}, m_{\tilde{\chi}_3^0}, m_{\tilde{\chi}_4^0}). \quad (48)$$

B.6 Vertex couplings

- Vertex $ig\gamma^\mu(g_{AB}^L P_L + g_{AB}^R P_R)$ [note that $g_{BA}^L = g_{AB}^{L*}$, $g_{BA}^R = g_{AB}^{R*}$]:

$$Z\tilde{\chi}_A^-\tilde{\chi}_B^- : \quad g_{AB}^L = \frac{1}{c_W} O_{AB}^{\prime L}; \quad O_{AB}^{\prime L} = \left(\frac{1}{2} - s_W^2\right) \mathbf{U}_{A2} \mathbf{U}_{B2}^* + c_W^2 \mathbf{U}_{A1} \mathbf{U}_{B1}^* \quad (49)$$

$$g_{AB}^R = \frac{1}{c_W} O_{AB}^{\prime R}; \quad O_{AB}^{\prime R} = \left(\frac{1}{2} - s_W^2\right) \mathbf{V}_{A2}^* \mathbf{V}_{B2} + c_W^2 \mathbf{V}_{A1}^* \mathbf{V}_{B1} \quad (50)$$

$$Z\tilde{\chi}_A^0\tilde{\chi}_B^0 : \quad g_{AB}^L = \frac{1}{c_W} O_{AB}^{\prime\prime L}; \quad O_{AB}^{\prime\prime L} = \frac{1}{2} (\mathbf{N}_{A4} \mathbf{N}_{B4}^* - \mathbf{N}_{A3} \mathbf{N}_{B3}^*) \quad (51)$$

$$g_{AB}^R = \frac{1}{c_W} O_{AB}^{\prime\prime R}; \quad O_{AB}^{\prime\prime R} = -O_{AB}^{\prime\prime L*} \quad (52)$$

- Vertex $igG_{XY}(p_1 + p_2)^\mu$ [note that $G_{YX} = G_{XY}^*$]:

$$Z\tilde{\nu}_X^\dagger\tilde{\nu}_Y : \quad G_{XY} = -\frac{1}{2c_W} \sum_{K=1}^3 \mathbf{S}_{XK}^{\tilde{\nu}} \mathbf{S}_{YK}^{\tilde{\nu}*} \quad (53)$$

$$Z\tilde{\ell}_X^\dagger\tilde{\ell}_Y : \quad G_{XY} = \frac{1}{c_W} \sum_{K=1}^3 \left[\left(\frac{1}{2} - s_W^2\right) \mathbf{S}_{XK}^{\tilde{\ell}} \mathbf{S}_{YK}^{\tilde{\ell}*} - s_W^2 \mathbf{S}_{X,K+3}^{\tilde{\ell}} \mathbf{S}_{Y,K+3}^{\tilde{\ell}*} \right] \quad (54)$$

- Vertex $ig(c_{IAX}^L P_L + c_{IAX}^R P_R)$:

$$\tilde{\nu}_X^\dagger \tilde{\chi}_A^- \ell_I : \quad c_{IAX}^{L[C]} = -\mathbf{V}_{A1}^* \mathbf{S}_{XI}^{\tilde{\nu}} \quad (55)$$

$$c_{IAX}^{R[C]} = \frac{m_{\ell_I}}{\sqrt{2} M_W \cos \beta} \mathbf{U}_{A2} \mathbf{S}_{XI}^{\tilde{\nu}} \quad (56)$$

$$\tilde{\ell}_X^\dagger \tilde{\chi}_A^0 \ell_I : \quad c_{IAX}^{L[N]} = \frac{1}{\sqrt{2}} (\tan \theta_W \mathbf{N}_{A1}^* + \mathbf{N}_{A2}^*) \mathbf{S}_{XI}^{\tilde{\ell}} - \frac{m_{\ell_I}}{\sqrt{2} M_W \cos \beta} \mathbf{N}_{A3}^* \mathbf{S}_{X,I+3}^{\tilde{\ell}} \quad (57)$$

$$c_{IAX}^{R[N]} = -\sqrt{2} \tan \theta_W \mathbf{N}_{A1} \mathbf{S}_{X,I+3}^{\tilde{\ell}} - \frac{m_{\ell_I}}{\sqrt{2} M_W \cos \beta} \mathbf{N}_{A3} \mathbf{S}_{XI}^{\tilde{\ell}} \quad (58)$$

C The LFV decay $\ell_J \rightarrow \ell_I \gamma$ and $g - 2$

The general amplitude $\ell_J \rightarrow \ell_I \gamma$ at one loop reads

$$\mathcal{M} = -ie \frac{\alpha_W}{4\pi} \varepsilon_\gamma^\mu \bar{u}_{\ell_I}(p_2) \frac{1}{m_{\ell_J}} [(i f_M^\gamma + f_E^\gamma \gamma_5) \sigma_{\mu\nu} q^\nu] u_{\ell_J}(p_1). \quad (59)$$

In the literature one finds often the notation:

$$\frac{\alpha_W}{4\pi} f_M^\gamma = \frac{m_{\ell_J}^2}{2} (A_2^L + A_2^R), \quad i \frac{\alpha_W}{4\pi} f_E^\gamma = \frac{m_{\ell_J}^2}{2} (A_2^L - A_2^R). \quad (60)$$

For equal leptons, the anomalous magnetic dipole moment of ℓ is

$$\delta a_\ell = \frac{g_\ell - 2}{2} = \frac{\alpha_W}{4\pi} f_M^\gamma = \frac{m_\ell^2}{2} (A_2^L + A_2^R). \quad (61)$$

The width of $\ell_J \rightarrow \ell_I \gamma$ is

$$\Gamma(\ell_J \rightarrow \ell_I \gamma) = \frac{\alpha \alpha_W^2}{32\pi^2} m_{\ell_J} (|f_M^\gamma|^2 + |f_E^\gamma|^2) = \frac{\alpha}{4} m_{\ell_J}^5 (|A_2^L|^2 + |A_2^R|^2). \quad (62)$$

Since the width $\Gamma(\ell_J \rightarrow \ell_I \nu_J \bar{\nu}_I) = \frac{G_F^2 m_{\ell_J}^5}{192\pi^3}$ and $G_F = \frac{\pi \alpha_W}{\sqrt{2} M_W^2}$, one has

$$\frac{\text{BR}(\ell_J \rightarrow \ell_I \gamma)}{\text{BR}(\ell_J \rightarrow \ell_I \nu_J \bar{\nu}_I)} = \frac{12\alpha}{\pi} \frac{M_W^4}{m_{\ell_J}^4} (|f_M^\gamma|^2 + |f_E^\gamma|^2) = \frac{48\pi^3 \alpha}{G_F^2} (|A_2^L|^2 + |A_2^R|^2), \quad (63)$$

where $\text{BR}(\ell_J \rightarrow \ell_I \nu_J \bar{\nu}_I) = 1/0.17/0.17$ for $\ell_J \ell_I = \mu e / \tau e / \tau \mu$, respectively.

The SUSY contribution to the form factors is:

- Diagram of type A: Chargino–Chargino–Sneutrino [$x_{AX} = m_{\tilde{\chi}_A^\pm}^2 / m_{\tilde{\nu}_X}^2$]:

$$\left. \frac{f_M^\gamma}{m_{\ell_J}} \right|_{\tilde{\chi}^\pm} = \sum_{A=1}^2 \sum_{X=1}^3 \left[\frac{m_{\ell_J}}{m_{\tilde{\nu}_X}^2} c_{IAX}^{L[C]*} c_{JAX}^{L[C]} F_1(x_{AX}) + \frac{m_{\tilde{\chi}_A^\pm}}{m_{\tilde{\nu}_X}^2} c_{IAX}^{L[C]*} c_{JAX}^{R[C]} F_2(x_{AX}) + L \leftrightarrow R \right] \quad (64)$$

$$i \left. \frac{f_E^\gamma}{m_{\ell_J}} \right|_{\tilde{\chi}^\pm} = \sum_{A=1}^2 \sum_{X=1}^3 \left[\frac{m_{\ell_J}}{m_{\tilde{\nu}_X}^2} c_{IAX}^{L[C]*} c_{JAX}^{L[C]} F_1(x_{AX}) + \frac{m_{\tilde{\chi}_A^\pm}}{m_{\tilde{\nu}_X}^2} c_{IAX}^{L[C]*} c_{JAX}^{R[C]} F_2(x_{AX}) - L \leftrightarrow R \right] \quad (65)$$

- Diagram of type B: Slepton–Slepton–Neutralino [$x_{AX}^0 = m_{\tilde{\chi}_A^0}^2 / m_{\tilde{\ell}_X}^2$]:

$$\left. \frac{f_M^\gamma}{m_{\ell_J}} \right|_{\tilde{\chi}^0} = \sum_{A=1}^4 \sum_{X=1}^6 \left[\frac{m_{\ell_J}}{m_{\tilde{\ell}_X}^2} c_{IAX}^{L[N]*} c_{JAX}^{L[N]} F_3(x_{AX}^0) + \frac{m_{\tilde{\chi}_A^0}}{m_{\tilde{\ell}_X}^2} c_{IAX}^{L[N]*} c_{JAX}^{R[N]} F_4(x_{AX}^0) + L \leftrightarrow R \right] \quad (66)$$

$$i \left. \frac{f_E^\gamma}{m_{\ell_J}} \right|_{\tilde{\chi}^0} = \sum_{A=1}^4 \sum_{X=1}^6 \left[\frac{m_{\ell_J}}{m_{\tilde{\ell}_X}^2} c_{IAX}^{L[N]*} c_{JAX}^{L[N]} F_3(x_{AX}^0) + \frac{m_{\tilde{\chi}_A^0}}{m_{\tilde{\ell}_X}^2} c_{IAX}^{L[N]*} c_{JAX}^{R[N]} F_4(x_{AX}^0) - L \leftrightarrow R \right] \quad (67)$$

where

$$F_1(x) = \frac{2 + 3x - 6x^2 + x^3 + 6x \ln x}{6(1-x)^4} \quad (68)$$

$$F_2(x) = \frac{-3 + 4x - x^2 - 2 \ln x}{2(1-x)^3} \quad (69)$$

$$F_3(x) = -\frac{1 - 6x + 3x^2 + 2x^3 - 6x^2 \ln x}{6(1-x)^4} = -xF_1(1/x) \quad (70)$$

$$F_4(x) = -\frac{1 - x^2 + 2x \ln x}{2(1-x)^3} \quad (71)$$

These functions are combinations of 3-point tensor integrals, in agreement with [36]:

$$F_1(x_{AX})/m_{\tilde{\nu}_X}^2 = 2 [C_{11} + C_{21} + C_{23}](0, 0, 0; m_{\tilde{\nu}_X}, m_{\tilde{\chi}_A^\pm}, m_{\tilde{\chi}_A^\pm}) \quad (72)$$

$$F_2(x_{AX})/m_{\tilde{\nu}_X}^2 = 2 C_{11}(0, 0, 0; m_{\tilde{\nu}_X}, m_{\tilde{\chi}_A^\pm}, m_{\tilde{\chi}_A^\pm}) \quad (73)$$

$$F_3(x_{AX}^0)/m_{\tilde{l}_X}^2 = -2 [C_{11} + C_{21} + C_{23}](0, 0, 0; m_{\tilde{\chi}_A^0}, m_{\tilde{l}_X}, m_{\tilde{l}_X}) \quad (74)$$

$$F_4(x_{AX}^0)/m_{\tilde{l}_X}^2 = [C_0 + C_{11} + C_{12}](0, 0, 0; m_{\tilde{\chi}_A^0}, m_{\tilde{l}_X}, m_{\tilde{l}_X}) \quad (75)$$

Note that the dipole form factors (64–67) are proportional to a fermion mass. The chirality flip takes place in the external fermion lines, for the terms proportional to LL and RR mixings and in the internal fermion lines (charginos or neutralinos), for the terms proportional to the LR mixing.

The branching ratio $\ell_J \rightarrow \ell_I \gamma$ reads

$$\begin{aligned} \text{BR}(\ell_J \rightarrow \ell_I \gamma) &= \text{BR}(\ell_J \rightarrow \ell_I \nu_J \bar{\nu}_I) \times \frac{12\pi\alpha\alpha_W^2}{G_F^2} \\ &\times \left\{ \left| \sum_{AX} \frac{1}{m_{\tilde{\nu}_X}^2} \left(c_{IAX}^{L[C]*} c_{JAX}^{L[C]} F_1(x_{AX}) + \frac{m_{\tilde{\chi}_A^\pm}}{m_{l_I}} c_{IAX}^{L[C]*} c_{JAX}^{R[C]} F_2(x_{AX}) \right) \right. \right. \\ &\quad \left. \left. \sum_{AX} \frac{1}{m_{\tilde{l}_X}^2} \left(c_{IAX}^{L[N]*} c_{JAX}^{L[N]} F_3(x_{AX}^0) + \frac{m_{\tilde{\chi}_A^0}}{m_{l_I}} c_{IAX}^{L[N]*} c_{JAX}^{R[N]} F_4(x_{AX}^0) \right) \right|^2 + L \leftrightarrow R \right\} \quad (76) \end{aligned}$$

References

- [1] M. L. Brooks *et al.* [MEGA Collaboration], Phys. Rev. Lett. **83**, 1521 (1999) [hep-ex/9905013].
- [2] K. W. Edwards *et al.* [CLEO Collaboration], Phys. Rev. D **55**, 3919 (1997).
- [3] S. Ahmed *et al.* [CLEO Collaboration], Phys. Rev. D **61**, 071101 (2000) [hep-ex/9910060].
- [4] U. Bellgardt *et al.* [SINDRUM Collaboration], Nucl. Phys. B **299**, 1 (1988).
- [5] D. W. Bliss *et al.* [CLEO Collaboration], Phys. Rev. D **57**, 5903 (1998) [hep-ex/9712010].

- [6] R. Akers *et al.* [OPAL Collaboration], Z. Phys. C **67**, 555 (1995).
- [7] P. Abreu *et al.* [DELPHI Collaboration], Z. Phys. C **73**, 243 (1997).
- [8] T. Yanagida, Prog. Theor. Phys. **64**, 1103 (1980), also in *Proceedings of the Workshop on the Unified Theory and the Baryon Number in the Universe*, Tsukuba, Japan, February 13-14, 1979, eds. A. Sawada and A. Sugamoto, p. 95, KEK Report 79-18;
M. Gell-Mann, P. Ramond and R. Slansky, in *Proceedings of the Workshop on Supergravity, Stony Brook, New York*, September 27-28, 1979, eds. P. van Nieuwenhuizen and D. Friedman (North-Holland, Amsterdam, 1979), p. 315-321;
R. N. Mohapatra and G. Senjanovic, Phys. Rev. Lett. **44**, 912 (1980).
- [9] J. I. Illana and T. Riemann, Phys. Rev. D **63**, 053004 (2001) [hep-ph/0010193];
J. I. Illana, M. Jack and T. Riemann, hep-ph/0001273.
- [10] D. Atwood, S. Bar-Shalom, G. Eilam, and A. Soni, hep-ph/0203200.
- [11] J. A. Aguilar-Saavedra *et al.* [ECFA/DESY LC Physics Working Group Collaboration], “TESLA Technical Design Report Part III: Physics at an e^+e^- Linear Collider”, hep-ph/0106315.
- [12] G. Wilson, talks at DESY-ECFA LC Workshops in Frascati, Nov 1998 and Oxford, March 1999.
- [13] J. Hisano, hep-ph/0204100.
- [14] M. J. Levine, Phys. Rev. D **36**, 1329 (1987).
- [15] M. Frank and H. Hamidian, Phys. Rev. D **54**, 6790 (1996) [hep-ph/9603222].
- [16] J. Hisano, T. Moroi, K. Tobe and M. Yamaguchi, Phys. Rev. D **53**, 2442 (1996) [hep-ph/9510309];
J. Hisano and D. Nomura, Phys. Rev. D **59**, 116005 (1999) [hep-ph/9810479];
S. w. Baek, T. Goto, Y. Okada and K. i. Okumura, Phys. Rev. D **64**, 095001 (2001) [hep-ph/0104146].
- [17] D. F. Carvalho, M. E. Gómez and J. C. Romao, Phys. Rev. D **65**, 093013 (2002) [arXiv:hep-ph/0202054].
- [18] D. Delepine and F. Vissani, Phys. Lett. B **522**, 95 (2001) [hep-ph/0106287].
- [19] M. Frank, Phys. Rev. D **65**, 033011 (2002).
- [20] I. Hinchliffe and F. E. Paige, Phys. Rev. D **63**, 115006 (2001) [hep-ph/0010086].
- [21] N. Arkani-Hamed, H. C. Cheng, J. L. Feng and L. J. Hall, Phys. Rev. Lett. **77**, 1937 (1996) [hep-ph/9603431];
J. Hisano, M. M. Nojiri, Y. Shimizu and M. Tanaka, Phys. Rev. D **60**, 055008 (1999) [hep-ph/9808410];
J. Kalinowski, in *Proc. of the APS/DPF/DPB Summer Study on the Future of Particle Physics (Snowmass 2001)* ed. R. Davidson and C. Quigg, hep-ph/0202043.
- [22] P. Langacker and M. Plumacher, Phys. Rev. D **62**, 013006 (2000) [hep-ph/0001204].
- [23] E. O. Iltan and I. Turan, Phys. Rev. D **65**, 013001 (2002) [hep-ph/0106068].

- [24] C. x. Yue, H. Li, Y. m. Zhang and Y. Jia, Phys. Lett. B **536**, 67 (2002) [hep-ph/0204153].
- [25] F. Gabbiani and A. Masiero, Nucl. Phys. B **322**, 235 (1989);
F. Gabbiani, E. Gabrielli, A. Masiero and L. Silvestrini, Nucl. Phys. B **477**, 321 (1996) [hep-ph/9604387].
- [26] D. E. Groom *et al.* [Particle Data Group Collaboration], Eur. Phys. J. C **15**, 1 (2000).
- [27] D. F. Carvalho, J. R. Ellis, M. E. Gómez and S. Lola, Phys. Lett. B **515**, 323 (2001) [hep-ph/0103256];
Z. Chacko and G. D. Kribs, Phys. Rev. D **64**, 075015 (2001) [hep-ph/0104317].
- [28] T. Moroi, Phys. Rev. D **53**, 6565 (1996) [Erratum-ibid. D **56**, 4424 (1996)] [hep-ph/9512396].
- [29] M. Knecht, A. Nyffeler, M. Perrottet and E. De Rafael, Phys. Rev. Lett. **88**, 071802 (2002) [hep-ph/0111059];
I. Blokland, A. Czarnecki and K. Melnikov, Phys. Rev. Lett. **88**, 071803 (2002) [hep-ph/0112117];
J. Prades, hep-ph/0108192v3.
- [30] H. N. Brown *et al.* [Muon $g-2$ Collaboration], Phys. Rev. Lett. **86**, 2227 (2001) [hep-ex/0102017].
- [31] G. 't Hooft and M. Veltman, Nucl. Phys. B **44**, 189 (1972).
- [32] G. Passarino and M. Veltman, Nucl. Phys. B **160**, 151 (1979).
- [33] T. Hahn and M. Pérez-Victoria, Comput. Phys. Commun. **118**, 153 (1999) [hep-ph/9807565].
- [34] G. J. van Oldenborgh and J. A. Vermaseren, Z. Phys. C **46**, 425 (1990).
- [35] T. Appelquist and J. Carazzone, Phys. Rev. D **11**, 2856 (1975);
A. Dobado, M. J. Herrero and S. Peñaranda, Eur. Phys. J. C **12**, 673 (2000) [hep-ph/9903211].
- [36] W. Hollik, J. I. Illana, S. Rigolin, C. Schappacher and D. Stöckinger, Nucl. Phys. B **551**, 3 (1999) [Erratum-ibid. B **557**, 407 (1999)] [hep-ph/9812298].